Radiation-induced apoptosis in human non-small-cell lung cancer cell lines is secondary to cell-cycle progression beyond the G2-phase checkpoint

M. STUSCHKE†‡*, A. SAK†‡, R. WURM†, B. SINN†, G. WOLF†, G. STÜBEN‡ and V. BUDACH†

Abstract.
Purpose: To characterize the relationship between cell-cycle progression and radiation-induced apoptosis in NSCLC cell lines with different p53 status.
Materials and methods: Cell lines with functional (H460, A549) and non-functional p53 (H661 and H520) were irradiated with 20 Gy. Multiparameter flow-cytometry was used to follow the progression of synchronized cells through the cell cycle after irradiation.
Results: Delayed apoptosis was observed after cell-cycle progression beyond the G2 block, either in the late G2/M-phase of the same cell cycle being irradiated (H661, H520) or in the G1-phase of the subsequent cell cycle (H460, A549). The apoptotic fraction in H661 and H520 was 60–80% at 144 h after irradiation, higher than in A549 and H460 (5 and 35%, respectively). As an alternative to apoptosis in cells cycling beyond the G2 restriction point, hyperploid cells were generated by all cell lines. Inhibition of cell-cycle progression through the G2/M-phase efficiently reduced the induction of late apoptosis. After irradiation in S-phase, 50–60% of cells with functional p53 remained arrested at the G2 restriction point until 144 h post-irradiation, while only 20% of the H661 or H520 did so.
Conclusions: These data characterize radiation-induced apoptosis in NSCLC cell lines as a removal pathway of clonogenically inactivated cells secondary to cell-cycle progression beyond G2/M, and is unlikely to be a critical factor for cellular radiation sensitivity.

1. Introduction

A basic question concerning radiation-induced apoptosis is whether apoptosis is only a secondary removal pathway of cells carrying residual DNA damage that leads to a loss of clonogenic capacity or whether apoptosis is directly triggered by potentially lethal damage to DNA or other targets that alternatively could be removed by other detoxifying pathways (Dewey *et al.* 1995, Olive and Durand 1997, Radford 1999).

Well-known apoptosis pathways mediated by p53, FAS/Apo-1/CD95 or sphingomyelin/ceramide (Zhivotovsky *et al.* 1999) lead to early apoptotic morphology within 12 h (Lowe *et al.* 1993, Jarvis *et al.* 1994, Bennet *et al.* 1998). With respect to radiation-induced apoptosis, the p53-mediated pathway was the first thought to be relevant in some cell types with high radiation sensitivity (Lowe *et al.* 1993, Clarke *et al.* 1994). Early radiation-induced apoptosis has been demonstrated in non-proliferating B- and T-lymphocyctes, myeloid progenitor cells, intestinal epithelia and differentiating spermatogonia with wild-type p53. In contrast to the sensitive p53 wild-type cells, the same cell types from the $p53^{-/-}$ mouse are much more resistant to the induction of early apoptosis within 12 h following irradiation (Clarke *et al.* 1993, Lotem and Sachs 1993, Lowe *et al.* 1993, Merrit *et al.* 1994, Hasegawa *et al.* 1998). Transfection of cDNA encoding for p53 in cells lacking this protein can restore the apoptotic response (Yonish-Rouach *et al.* 1991). In addition, the FAS/Apo-1/CD95 and sphingomeylin pathways can also play a role in early radiation-induced apoptosis in certain cell types (Haimovitz-Friedman *et al.* 1994, Santana *et al.* 1996, Herr *et al.* 1997, Belka *et al.* 1998, Pena *et al.* 2000). In endothelial cells, genetic mutations of acid sphingomyelinase that inactivate the sphingomyelin/ceramide pathway can lead to a marked reduction in ionizing radiation-induced early apoptosis (Pena *et al.* 2000).

Radiation-induced p53-dependent early apoptosis is physiologically expressed in normal epithelial cells from some but not all tissues, e.g. the skin (Uberti *et al.* 1999). In contrast to early apoptosis, epithelia from all studied tissues showed late apoptosis at 24 h or more after irradiation (Uberti *et al.* 1999), which was p53-independent and which demonstrates that radiation-induced late apoptosis is a general phenomenon in epithelia in comparison with the p53-dependent early apoptosis. The knowledge of mechanisms leading to late p53-independent radiation-induced apoptosis is rather limited. Strasser

*Author for correspondence;
e-mail: martin.stuschke@uni-essen.de
†Department of Radiotherapy, Humboldt-University, Charité, D-10117 Berlin, Germany.
‡Present address: University of Essen, Department of Radiotherapy, Hufelandstr. 55, D-45122 Essen, Germany.

et al. (1994) observed that proliferation is an important prerequisite for p53-independent late apoptosis after irradiation in $p53^{-/-}$ lymphoid cells. Merrit *et al.* (1997) also showed an association between radiation-induced late apoptosis in small intestinal epithelia from the $p53^{-/-}$ mouse and cell-cycle progression beyond the radiation-induced G2-phase block, pointing to a dependence of late apoptosis on cell-cycle progression. It has been shown that the G2 block following DNA damage by ionizing radiation can be prolonged by a p53-mediated pathway leading to transcription of 14-3-3$_\sigma$ and $p21^{WAF1/CIP1}$, which prevents the activation of the cdc2-cyclinB1 complex (Chan *et al.* 1999). In cells where this pathway is disrupted, cdc2 and cyclin B1 can enter the nucleus and lead to a premature entry into mitosis, eventually leading to a mitotic catastrophe, i.e. an apoptotic-like process beginning in the prophase (Chan *et al.* 1999).

Non-small-cell lung cancer (NSCLC) is the most common cause of cancer death in men (Fry *et al.* 1999) and radiotherapy has a firm position as a component of standard therapy in locally advanced NSCLC. Up to now, radiation-induced apoptosis was measured in only a few NSCLC cell lines (Perdomo *et al.* 1998, Sirzen *et al.* 1998). In both studies, NSCLC cell lines did not show sustained radiation-induced apoptosis. Regarding radiation-induced apoptosis in all tumour types, early apoptosis within 12–24 h after irradiation was seldom observed in cells from solid tumours. Stapper *et al.* (1995) observed early radiation-induced apoptosis within 24 h after irradiation in only two of six sarcoma cell lines but not in 14 human glioma cell lines. In the former two, early radiation-induced apoptosis occurred only in 8–15% of cells at high doses of 25 Gy leading to inactivation of the ability to form colonies in >99.9% of cells. Meyn *et al.* (1993) did not find early radiation-induced apoptosis in five murine sarcomas and three squamous cell carcinoma cell lines but in the majority of murine mammary adenocarcinomas. In cells from epithelial tumours, radiation-induced apoptosis occurs preferentially late (Bracey *et al.* 1995, 1997, Yanagihara *et al.* 1995). By far the most apoptotic cells occurred later than 24 h after irradiation. This late apoptosis was also inducible in $p53^{-/-}$ adenocarcinoma cell lines and showed a temporal relationship to the exit from radiation-induced G2-phase arrest (Bracey *et al.* 1995).

The aim was to determine whether apoptosis can be induced in human NSCLC cancer cell lines with functionally active or inactive p53 to a relevant amount and whether induction of radiation-induced apoptosis is an early event after irradiation or a late downstream event which can be modulated by intervening steps.

2. Materials and methods

2.1. *Cell culture*

The NSCLC cell lines H460, H661 and H520 were obtained from the American Type Culture Collection (ATCC, Rockville, MD, USA) and were grown in RPMI 1640 containing 10% foetal calf serum. The NSCLC cell line A549 was obtained from DSZM (Braunschweig, Germany) and grown in Eagle's minimal essential medium (MEM) supplemented with 15% foetal calf serum. Both media were supplemented with non-essential amino acids, penicillin/streptomycin (100 units ml^{-1}, all Gibco-BRL, Paisley, UK). Cultures were irradiated using a ^{60}Co source at a dose-rate of 1.9 Gy min^{-1}. Control cells were sham irradiated.

2.2. *Synchronization of cells*

Cells were synchronized by release from confluence. Accumulation of tumour cells in plateau-phase was achieved through serum starvation and contact inhibited growth. This resulted in an equilibrium number of approximately 10^5 cells cm^{-2} for H661 and $3–5 \times 10^5$ cells cm^{-2} for H460, H520 and A549 cells with 75–90% in G1, 2–10% in S and 10–15% in G2/M. After subculture of plateau-phase cells with a cell density of 0.2×10^5 cells cm^{-2} for H661 and 0.4×10^5 cells cm^{-2} for the other cell lines, cells were irradiated either 5 or 20–25 h post-subculture for populations enriched in early G1- or S-phase, respectively. Depending on the cell lines used, S-phase-enriched populations at 20–25 h post-subculture consisted of about 30–50% cells in late G1, 30–50% in S and 10–15% in G2/M.

2.3. *BrdU/Hoechst quenching technique*

A BrdU/Hoechst quenching technique was used for measurements of cell-cycle progression after irradiation by flow-cytometry (Gilligan *et al.* 1996). Briefly, cells were continuously labelled with an equimolar concentration of 40 μM 5-bromo deoxyuridine and deoxycytidine (BrdU, Sigma, Deisenhofen, Germany) directly after irradiation. Cell cultures were harvested at various times between 0 and 144 h after irradiation. Bivariate BrdU/Hoechst-EB cytograms were measured with a PAS-II flow-cytometer (Partec AG, Münster, Germany) using UV light (HBO 100 mercury lamp) for excitation at 365 nm and emission filters for measuring red fluorescence of EB (570 nm) and blue fluorescence of Hoechst

33258 (435 nm). A final display of red (EB) versus blue (Hoechst 33258) was produced. Figures were prepared using the WINMDI software (Joe Trotter, Salk Institute, La Jolla, CA, USA). For each cytogram, regions corresponding to the cell cycle compartments were defined according to Gilligan *et al.* (1996) and the number of cells determined for calculation of the percentage of cells in each compartment. Irradiated cells in G1- and early S-phases can be followed into the G2-phase (G2f) of the first cell cycle (i.e. the cell cycle in which the cells were irradiated), and eventually to the next G1 (G1′)- or G2 (G2′)-phases of the second cell cycle (i.e. the next cell cycle after irradiation).

2.4. *Analysis of DNA synthesis*

Cells were continuously labelled with 40 μM BrdU (Roche Molecular Biochemicals, Mannheim, Germany) which was added at 0 or 72 h after radiation to the medium. At 144 h after irradiation, cells were harvested, washed and fixed in 70% ethanol. Subsequently, cells were washed with PBS and treated with 0.1% RNAse for 15 min. After denaturation of DNA with 4 N HCl for 20 min, cells were neutralized to pH 7.4 with 0.1 M sodium tetraborate (pH 8.5), then stained with fluorescein isothiocyanate (FITC)-conjugated anti-BrdU monoclonal antibody (Roche Molecular Biochemicals, Mannheim, Germany), washed and stained for DNA with 5 μg ml^{-1} PI. Approximately 10^6 cells were resuspended in 1 ml PBS and analysed on a flow cytometer for green fluorescence (BrdU) versus red fluorescence (DNA).

To study DNA synthesis by ^{3}H incorporation, cells were incubated with 3.7 kBq ml^{-1} [methyl-^{3}H]-thymidine (3.11 TBq mmol^{-1}) (Amersham, Freiburg, Germany) at 0 or 24 h after irradiation for 90 min under an atmosphere of 5% $C0_2$ and 95% air at 37°C. Thereafter radioactivity was washed out and cells were incubated in fresh medium without radioactivity, containing 0.23×10^3 mol l^{-1} thymidine. Apoptotic cells (detached) and non-apoptotic (attached) cells were recovered and radioactivity determined.

2.5. *Preparation of metaphase cells*

Cells were irradiated with 20 Gy at 20–24 h after the release from the plateau-phase by subcultivation. Detached cells and adherent cells were collected separately at 48, 72, 96 or 120 h post-irradiation. Cell preparations were made by dropping the hypotonically swollen cell suspension onto clean slides wetted with ice-cold distilled water. The slides were stained with 10% Giemsa, air dried and coated with Entellan (Merck, Darmstadt, Germany). Assessment and determination of mitotic figures was done by Ikarus software (Metasystems) at a 1000 × magnification. Scoring of aberrant mitotic figures, i.e. spontaneous premature chromosome condensation (SPCC), and metaphases with fragmented and pulverized chromosomes, was performed on a Leitz microscope (Leitz, Wetzlar, Germany).

2.6. *Measurement of apoptosis*

2.6.1. *Hoechst-33342 staining.* To visualize apoptosis in monolayer cultures, Hoechst-33342 (Sigma) was added to the culture medium to give a final concentration of 1.0 μg ml^{-1}, then 20 min later PI solution was included to 5 μg ml^{-1}. The total number of apoptotic cells included those found floating in the medium and those in the adherent fraction were counted according to Stapper *et al.* (1995). The fraction of apoptotic cells (A) in the whole cell population was determined according to:

$$A = (A_f + A_a)/(f + a),$$

where A_f and A_a are the number of apoptotic cells in the floating and adherent fractions, and f and a are the number of cells (apoptotic and non-apoptotic) in the floating and adherent fractions.

2.6.2. *Flow-cytometric analysis of DNA fragmentation.* During apoptosis, reduced fluorescence with respect to the G0/G1 cell-cycle region (sub-G1 region) can be detected when apoptotic cells are analysed by flow-cytometry. Thus, the presence of fluorescence in the sub-G1 region can be used as a marker of apoptosis. The sub-G1 region was determined in flow-cytometry by a gate defined in the controls excluding the debris at the origin of the abscissa and ending at the beginning of the G1 peak.

2.6.3. *F-actin staining.* As a third method for detecting apoptosis, the loss of cell surface structures such as pseudopodia and microvilli was used for discrimination of apoptotic cells in flow-cytometry and detection of their cell cycle specificity as described elsewhere (Endresen *et al.* 1995). Analytic flow-cytometric measurements of cells were performed using a PAS-II flow-cytometer (Partec AG, Münster, Germany) with argon laser excitation at 488 nm and detection of red fluorescence (PI, DNA) at 630 nm versus green fluorescence (F-actin) at 520 nm. The morphological analysis of Hoechst 33342/PI stained cells was the most gentle and most sensitive method to detect highly fragile apoptotic cells with minimal cell loss, followed by the morphological assessment of the F-actin signal.

2.7. *Modulation of G2/M transition and DNA repair by drug treatment*

Genistein (Sigma) was dissolved in DMSO at a concentration of 20 mM and stored at −20°C until used. To observe the effect of genistein on cell-cycle progression and apoptosis, 25 μM (for H460) and 30 μM (for H520 and H661) was added to the culture medium just after irradiation with 20 Gy. Wortmannin (Sigma), dissolved at a concentration of 5 mM in DMSO was added to the culture medium 1 h before irradiation.

2.8. *Clonogenic survival assay*

For the measurement of clonogenic survival, plateau-phase cells were harvested and plated in triplicate in 25-cm^2 T-flasks (Nunc, Wiesbaden Germany). After 5 h in culture, cells were irradiated and incubated at 37°C in 5% CO_2 for 10–14 days. Cells were washed with PBS, fixed with 96% ethanol and stained with 15% (w/v) Giemsa and destained with distilled water. Colonies were counted that had >50 cells or had a diameter >100 μm. The surviving fractions after a radiation dose of 2 Gy (SF2) are presented as a fraction of the growth of untreated colonies.

2.9. *Inhibition of anchorage-dependent growth*

To obtain cells cultured under non-adherent conditions, S-phase-enriched cell suspensions were trypsinized immediately after irradiation and seeded in 9.6 cm^2 culture plates coated with 2 ml 1% (w/v) high melting point agarose in PBS/culture medium (1:1). The same aliquots were seeded in tissue culture plates without agarose as controls. Cells on agarose had no anchorage to plastic and grew as cell aggregates. Cells were serially sampled at 48, 72 and 144 h post-irradiation and treated with accutase (PAA Laboratories, Vienna, Austria) to obtain a single-cell suspension. Cells were centrifuged, resuspended in HBSS containing Hoechst-33342 (Sigma), and stained for 30 min at 37°C. The fraction of apoptosis was determined according to the morphological criteria. For cell-cycle analysis, cells continuously labelled with BrdU just after irradiation, were treated with accutase, spun and resuspended in culture medium containing 10% DMSO, and stored at −80°C in medium until required for analysis.

2.10. *Measurement of protein expression*

Nuclear extracts were prepared according to Tishler *et al.* (1993). Expression of the proteins p53, $p21^{WAF1/CIP1}$ and Bcl-2 was measured in nuclear extracts according to the instructions of the supplier, using pantropic ELISA immunoassay kits (Calbiochem, Bad-Soden, Germany) specific for p53 (QIA 26), p21 (QIA18) and Bcl-2 (QIA23), respectively.

2.11. *Screening for p53 mutations by TGGE and sequencing*

Temperature gradient gel electrophoresis (TGGE) and sequencing of fragments containing one of the exons 5, 6, 7 and 8 of the p53 gene were done according to Schlechte *et al.* (1997). Briefly, sequences were amplified by PCR and TGGE was run in 8% polyacrylamide gels. Sequence analysis was done by solid-phase DNA sequencing of amplified genomic DNA and a laser-fluorescent electrophoresis unit. The wild-type sequence of the human p53 gene was used as reference.

2.12. *Induction and repair of DNA double-strand breaks*

Uniformly labelled cells (1.85 kBq [2-^{14}C]-thymidine ml^{-1} (1.92 MBq $mmol^{-1}$) for 72 h were subcultured to low density of $0.5–1 \times 10^5$ cells cm^{-2} and irradiated 20 h later with 30 Gy. Cells were sampled at 0 and 4 h post-irradiation and cast into plug moulds. Plugs were transferred into lysis buffer (100 mM EDTA, 10 mM Tris, 20 mM NaCl, 1 mg ml^{-1} proteinase K, 1%(w/v) sodium lauryl sarcosine, pH 8.0) and incubated for 24 h at 50°C. Plugs were then washed and cut into 5-mm pieces containing approximately 1 μg DNA. For electrophoresis, plugs were loaded into wells of 0.75% agarose. Electrophoresis was carried out in 0.5 × TBE buffer (45 mM Tris borate, 1 mM EDTA, pH 8.0) at room temperature for 72 h at a constant field strength of 0.6 V cm^{-1}. After staining with ethidium bromide, the wells and each lane of the gel were cut into separate segments and radioactivity determined. The fraction of radioactivity released from the plugs into the gels (FAR) was calculated using:

$$\text{FAR} = (\text{dpm in the lane})/(\text{dpm in the lane} + \text{dpm in the well}).$$

2.13. *Data evaluation*

All experiments were repeated at least three times, and the data are given as a mean ± SEM for the independent experiments. Statistical analysis (two-sided *t*-test) and graphs were performed with the aid of Microcal Origin version 4.1 (Microcal Software, Northampton, MA, USA).

3. Results

3.1. *Clonogenic survival, and expression of genes with relevance to apoptosis*

Clonogenic survival, apoptosis and expression of p53, $p21^{WAF1/CIP1}$ and Bcl-2 were determined in four NSCLC cell lines. The p53 status was analysed using wild-type and mutant specific antibodies in ELISA tests and with temperature-gradient gel-electrophoresis (TGGE) of exons 5, 6, 7 and 8 with subsequent sequencing. In addition, radiation-induced expression of p53 and $p21^{WAF1/CIP1}$ proteins as a functional test and clonogenic survival at a radiation dose of 2 Gy (SF2) was defined. These data are summarized in table 1. Of the four cell lines studied, two (H460, A549) have a wild-type p53 sequence and functional with respect to radiation-induced expression of the p53 and $p21^{WAF1/CIP1}$ proteins. In H661 cells, p53 was mutated according to sequence analysis by TGGE and functional inactive with respect to radiation-induced expression of p53 and $p21^{WAF1/CIP1}$. H520 cells were functional inactive for p53, although we failed to detect p53 mutation, both with mutant specific antibodies and TGGE analysis of exons 5–8. Expression of the Bcl-2 protein was by a factor of about two higher in the cell lines H460 and A549 in comparison with H661 and H520 cells.

3.2. *Cell-cycle progression following irradiation*

Cells synchronized by serum starvation in the G1-phase with a G1 fraction of 80–90%, were irradiated with 20 Gy, either at 5 h (early G1-phase) or 20–24 h (maximal S-phase) after subculture in fresh medium and cell-cycle progression was analysed using the BrdU-Hoechst quenching technique of Gilligan *et al.* (1996). The high irradiation dose of 20 Gy ensured a homogeneous population with severe radiation damage, so that an overgrowth by clonogenically active cells did not occur. In fact, the total number of cells in culture did not change by more than a factor of 1.5 after irradiation.

Figure 1 summarizes the cell-cycle progression of H460 (a) and H661 (b) cell lines irradiated with 20 Gy in S-phase of the cell cycle. The cell cycle profiles of A549 and H520 cells after irradiation with 20 Gy in S-phase were similar to those of H460 and H661, respectively (data not shown). At 24 h after irradiation of S-rich populations, all cell lines studied showed a delay in the G2/M-phase of the cell cycle (figure 1). The duration of the G2-phase block, however, was much more pronounced in A549 and H460 with functional p53, in comparison with H520 and H661 with non-functional p53. The percentage of cells in the G2/M-phase at 24 h after irradiation with 20 Gy increased from 17.0 ± 1.5, 13.0 ± 1.7, 12.0 ± 3.4 and 11.7 ± 5.9% to $61.5 + 2.5$, 69.8 ± 2.1, 76.1 ± 7.1 and 71.7 ± 3.3% in A549, H460, H520 and H661 cells, respectively. Cell lines with a wild-type p53 (A549, H460) heavily irradiated with 20 Gy showed an extended G2 cell cycle delay with a half-time of release of about 120 h in comparison with sham-irradiated controls with a half-time of release of 5 h. Cell lines with non-functional p53 (H661, H520) showed shorter G2-phase delays with a half-time of release of about 48 h in comparison with the sham-irradiated controls with a half-time of release of about 7 h. By 48 h a considerable number of cells from the p53-incompetent cell lines had completed the cell cycle and reached the new G1 (G1′), eventually the next G2 (G2′) or develop into cells with a hyperploid DNA content (>G2-phase) or had accumulated in the sub-G1 compartment. By 144 h only 20% of the A549 and 40% of the H460 cells, including sub-G1′ cells, stemmed from cells that have passed the G2/M block of the first cell cycle, while 80% of H661 and H520 cells did so.

For completeness, experiments were performed in G1 to monitor the progression of heavily irradiated cells through the whole cell cycle and beyond G2/M before the onset of apoptosis. Cell lines with

Table 1. Comparison of p53 status, protein expression, clonogenic survival and apoptosis in NSCLC cell lines.

Cell lines	TP53 status[1]	TP53 expression[2] 4 h after 6 Gy	p21 expression[3] 4 h after 6 Gy	Bcl-2 expression[4]	SF2 (%)[5]	Apoptosis (%)[6]
A549	wt	+	+	+ +	64.6 ± 4.3	4.0 ± 2.0
H460	wt	+	+	+ +	43.7 ± 2.8	30.8 ± 0.8
H520	wt	−	−	+	35.5 ± 4.4	79.7 ± 3.3
H661	mt	−	−	+	58.6 ± 5.3	57.0 ± 8.5

1, p53 status; wt, wild-type; mt, mutant. 2, Ionizing radiation-induced expression of p53 at 4 h after 6 Gy; (+) expression, (−) no expression. 3, Ionizing radiation-induced expression of $p^{21WAF1/CIP1}$ at 4 h after 6 Gy; (+) expression, (−) no expression. 4, Expression of Bcl-2 protein; (+) 4–5 U per 10^6 cells, (+ +) 10–20 U per 10^6 cells. 5, SF2, surviving fraction after 2 Gy. Data are the means ± SEM of three to five experiments. 6, Percentage of apoptosis 6 days after irradiation with 20 Gy. Data are mean ± SEM of at least five experiments.

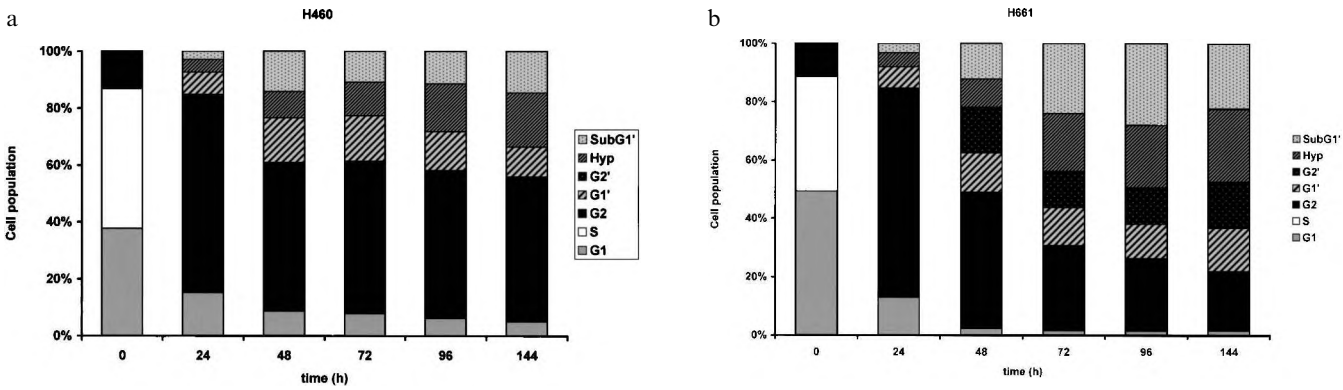

Figure 1. Time-course of cell-cycle progression of the cell lines H460 (a) an H661 (b) following irradiation with 20 Gy in the S-phase as an example for cell lines with functional and non-functional p53, respectively. The different phases of the first cell cycle (G1, S, G2) and those of the second cell cycle (G1′, G2′, Hyp, sub-G1′) are shown. G2 cells comprise both BrdU-labelled (G2f) and -unlabelled (G2) cells. Means of about four independent experiments are shown.

functional p53 irradiated in early G1-phase (figure 2) took longer to progress through the G1-phase than cells with inactive p53 with a half-time of release of about 96 h in comparison with sham-irradiated controls with a half-time of release of about 8 h. These cells also showed a longer delay at the first G2-phase (G2f). A fraction of about 50% of A549 and 20% of H460 remained in G1 of the first cell cycle until the end of the observation period, probably terminally arrested, while cell lines with non-functional p53 did not show any G1 arrest. The fraction of cells which has passed beyond the G2 block of the first cell cycle at the end of the follow-up period were the same for cells irradiated either in the G1- or in the S-phases.

As shown in figures 1 and 2, ionizing radiation led to a considerable number of cells with a hyperploid DNA content (>G2-phase). The fractions of hyperploid cells at 96 h after irradiation in S-phase were $7.0 \pm 0.6\%$, $16.8 \pm 4.1\%$, $18.7 \pm 1.2\%$ and $21.4 \pm 1.4\%$ for A549, H460, H520 and H661, respectively. The respective values for irradiating in G1-phase were $6.0 \pm 1.0\%$, $12.2 \pm 0.4\%$, $33.5 \pm 1.3\%$ and $38.0 \pm 5.6\%$. The hyperploid fraction of H661 and H520 cells was significantly higher after irradiating in the G1-phase than in S-phase ($p < 0.01$). However, the fraction of hyperploid cells in cell lines with functional p53 remained the same, irrespective of the cell-cycle phase of irradiation. In conclusion, these data show that cell-cycle progression of irradiated NSCLC cell lines was delayed in the G2-phase for all cell lines or in the G1-phase for cell lines with functional p53 irradiated in G1. Cell-cycle progression beyond the G1 and G2/M-phases, therefore depends on the p53 status of the cell lines.

3.3. *Expression of nuclear aberrations in irradiated cells before the onset of apoptosis*

Cell morphology in metaphase of detached cells at 120 h following irradiation with 20 Gy was examined. Figure 3 shows in addition to a normal metaphase of H520 (a), metaphases with hyperploidy

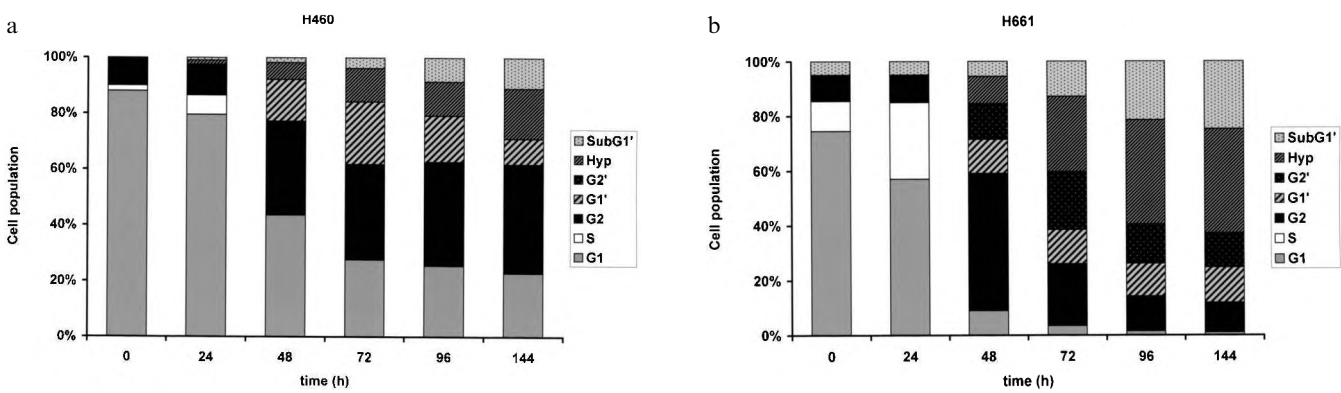

Figure 2. Time-course of cell-cycle progression of the cell lines H460 (a) and H661 (b) following irradiation with 20 Gy in the G1-phase as an example for cell lines with functional and non-functional p53, respectively. Means of about four independent experiments are shown.

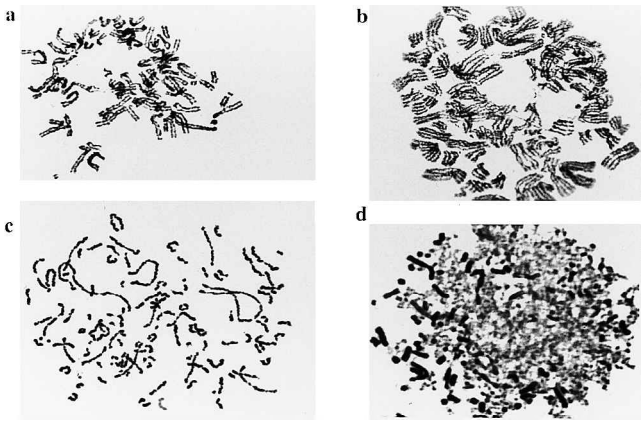

Figure 3. Chromosome preparations of H520 cells at 120 h following irradiation with 20 Gy. In addition to a normal metaphase (a), metaphases with a hyperploid number of chromosomes (b), with premature condensation of chromosomes (c) and with fragmented and pulverized chromosomes are shown. Detached cells were fixed, dropped on slides, stained with Giemsa and photographed (1000×).

resulting from endomitosis (b), spontaneous chromosome condensation (c) and fragmented or pulverized chromosomes (d). Additional experiments with fluorescence *in-situ* hybridization (FISH) technique were done and confirmed the existence of hyperploid cells (data not shown). Cells with spontaneous chromosome condensation (SPCC) and irregular fragmented or pulverized chromosomes are hallmarks of mitotic catastrophe. The maximum fraction of cells showing mitotic catastrophe at day 5 post-irradiation with 20 Gy was at about 30% in cell lines with non-functional p53, but was not observed in the cell lines H460 and A549 with functional p53.

3.4. *Relation between cell-cycle progression and induction of apoptosis*

The morphologic assessment of Hoechst-33342 stained cell suspensions was most sensitive and taken as reference method for the detection of radiation-induced apoptosis. The time-course for the development of apoptosis in the four cell lines irradiated either in S- or in G1-phase according to morphological criteria is shown in table 2. H460 cells irradiated in G1 showed a delayed and reduced induction of apoptosis, in comparison with irradiation of S-rich populations. Cell lines with functional p53 (H460, A549) irradiated in S-phase showed a reduced induction of apoptosis, in comparison with the cell lines with non-functional p53 (H661 and H520). This delayed and reduced induction of apoptosis of H460 cells irradiated in G1 was concomitant to the delay in cell-cycle progression with a pronounced block in G1- and G2/M-phases. Induction of apoptosis in H520 and H661 cells irradiated in early G1, in comparison with irradiation in S-phase was first delayed but reached the same level at later times post-irradiation. These data show that the onset of apoptosis appears to be preceded by a period of radiation-induced G2-phase block.

3.5. *Influence of residual DNA double-strand breaks on induction of apoptosis*

Repair inhibition experiments were performed to further analyse whether apoptosis tolerance dominated by cell-cycle progression could be bypassed by a dramatically increased prevalence of radiation-induced DNA damage. For these experiments, we chose the two cell lines with the least onset of apoptosis, A549 and H460. Cells in exponential growth were irradiated with 30 Gy and the fraction of DNA released (FAR) was determined immediately or after repair incubation for 4 h. In the presence of wortmannin, the fraction of mobile DNA at 4 h after irradiation which represents the fraction of residual DNA double-strand breaks, increased from 10% to about 60% in A549 and from 10% to about 50% in H460 cells. Despite the increase in residual damage, neither the fraction of apoptosis at 144 h post-irradiation of S-phase enriched populations measured by the morphologic method nor cell-cycle progression through G2/M was not influenced by wortmannin (data not shown).

3.6. *Direct analysis of the cell-cycle phase from which radiation-induced apoptosis appears*

To determine the cell-cycle phase from which apoptotic cells appear, bivariate analysis of F-actin and DNA content have been evaluated in the same cell by flow-cytometry. Figure 4 shows bivariate dot plots of red fluorescence (DNA) versus green fluorescence (F-actin) of H460 and H661 cells at 24, 72 and 144 h post-irradiation with 20 Gy in S-phase. The F-actin negative population of H460, representing the apoptotic fraction, appeared from cells with G1 DNA content. At 144 h the DNA content of the F-actin negative population shifted towards S- and G2/M-phases. This phenomenon was further analysed using apoptotic cells from the supernatants, which were incubated for different time intervals in culture medium. The shift towards G2/M-phase was the result of increased DNA staining with propidium iodide due to a loss of membrane integrity of apoptotic cells, which did not lose DNA at this time. In comparison, the F-actin negative population of H661 (figure 4) and H520 cells (data not shown) developed from G2-phase cells and later shifted towards G1

Table 2. Time-course of morphologically determined apoptosis following irradiation of NSCLC cell lines with 20 Gy in S-and G1-phase.

Cell lines	24 h	48 h	72 h	96 h	144 h
A549					
S-phase	0.3±0.3	1.0±0.0	1.7±0.7	2.3±0.9	4.0±2.0
G1-phase	1.5±0.5	0.5±0.5	2.0±0.1	3.0±0.1	4.5±0.5
H460					
S-phase	6.0±1.5	24.8±2.4	27.3±4.6	35.0±6.2	30.8±0.8
G1-phase	2.3±0.2	1.3±0.3	2.5±0.4	8.8±1.6	10.2±2.0
H520					
S-phase	3.0±2.0	5.7±0.9	11.8±2.2	44.3±4.6	79.7±3.3
G1-phase	1.5±0.5	3.5±0.5	5.0±1.0	22.5±3.9	79.5±1.5
H661					
S-phase	2.3±0.9	13.3±0.8	24.8±4.0	38.3±3.6	57.0±8.5
G1-phase	2.7±0.2	2.6±0.5	10.1±1.2	42.8±5.1	59.0±4.7

Data are means±SEM of three to six experiments.

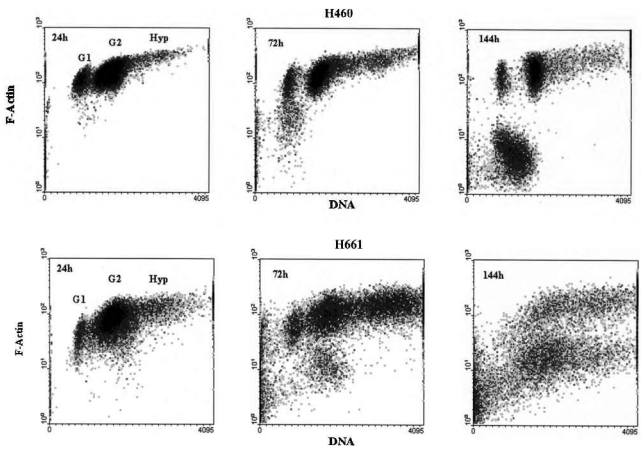

Figure 4. Bivariate dot plots of green (FITC-phalloidin, F-actin) versus red fluorescence (PI, DNA) of H460 and H661 at 24, 72 and 144 h following irradiation with 20 Gy in S-phase. Regions corresponding to the cell cycle compartments were defined with G1, G2 and Hyp (hyperploid cells) with F-actin negative population representing the apoptotic fraction. The F-actin negative cells result from different populations, either from G1 (H460) or from G2 and from hyperploid cells (H661).

and sub-G1 due to the loss of DNA from apoptotic cells. The hyperploid population of H661 and H520 cells became also F-actin negative at 144 h. However, hyperploid H460 and A549 cells remained F-actin positive and therefore did not apoptose during the observation time.

From these experiments alone, it cannot be distinguished whether the onset of apoptosis in H460 is from the G1-phase of the first cell cycle or the second cell cycle with respect to irradiation (G1′). Therefore, additional experiments were performed with H460 cells, which were pulse-labelled for 90 min with ^{3}H-thymidine at 0 or 24 h after irradiation. The amount of ^{3}H-thymidine incorporated into the DNA of apoptotic cells was by a factor of 50 higher if cells were pulsed-labelled at the time of irradiation (0 h) than at 24 h after irradiation. Apoptotic H460 cells with a G1 DNA content therefore originate from S-phase cells at the time of irradiation and stem from G1′-phase and not from a subpopulation of G1-phase cells among the synchronized cells at the time of irradiation, that remained blocked in G1.

To analyse further whether H661 cells can progress through the S′-phase of the second cell cycle after irradiation before the onset of apoptosis, cells were labelled with BrdU at different times post-irradiation. BrdU was given either directly (0 h) or at 72 h after irradiation of S-phase enriched populations with 20 Gy. At 144 h after permanent BrdU labelling from 0 h after irradiation, the fraction of the apoptotic (sub-G1) cells which show positive BrdU staining e.g. was at about 75% for H661 cells. In comparison, if BrdU was applied at 72 h post-irradiation the fraction of BrdU positive sub-G1 cells reduced to 7%. These data show that the vast majority of apoptotic H661 and H520 cells primarily originate from the G2/M-phase of the first cell cycle.

3.7. *Modulation of cell-cycle progression by genistein and cell–matrix interaction and the consequences for the generation of apoptoses*

To analyse further the necessity of G2/M-phase transition for the onset of radiation-induced late apoptosis, progression of cells through the G2/M-phase was delayed with genistein. Initially, the dose–response effect of genistein was studied to identify a concentration that would effectively inhibit the G2/M-transition cells with minimal toxicity (<10% cell death at 144 h) in non-irradiated cells. Treatment of irradiated cell lines with 30 μM genistein increased

the fraction of G2/M-phase cells from 25.2±0.3% to 65.7±2.7% in H520 ($p<0.001$, figure 5) and from 25.0±2.5% to 41.3±4.0% in H661 ($p<0.05$, data not shown) at 96 h following irradiation. The fraction of apoptosis measured by Hoechst 33342 staining was also significantly ($p<0.01$) reduced by 45 and 50% of that observed in cultures irradiated without genistein (figure 6). The augmented G2 block and decreased generation of apoptoses has been shown to be reversible by washing out genistein from the culture medium 24 h post-treatment. An effect of genistein on G2 block and appearance of apoptoses in cell lines with functional p53 (H460, A549) was not detectable (data not shown). These data demonstrate that the mechanism of delayed apoptosis is mainly controlled by cell-cycle progression through the G2/M-phase.

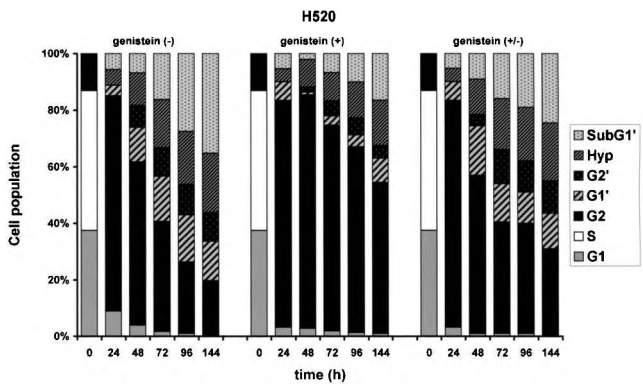

Figure 5. Time-course of cell-cycle progression in H520 treated with 30 μM (+) and without genistein (−) just after irradiation with 20 Gy in S-phase and after washing out genistein from the cell culture medium at 24 h post-irradiation (+/−). Means of four independent experiments are shown.

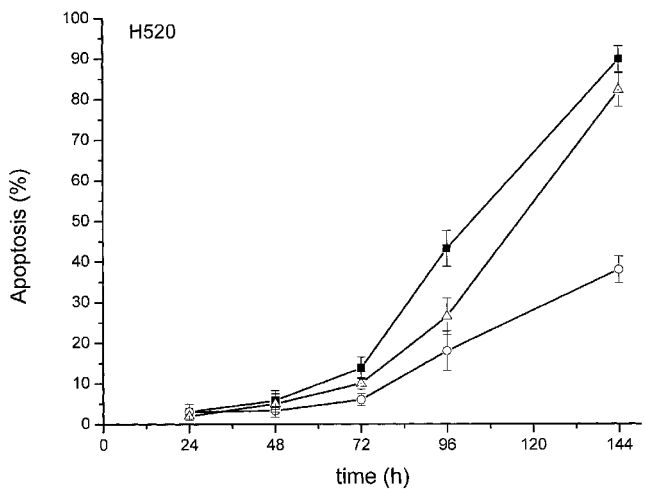

Figure 6. Time-course of apoptosis in H520 cells following irradiation with 20 Gy in S-phase, treated with (○) and without (■) genistein and after washing out genistein from the cell culture medium at 24 h post-irradiation (△). Means±SEM of at least four independent experiments are shown.

To test the a hypothesis that genistein suppresses cell-cycle progression by a p53-independent expression of $p21^{WAF1/CIP1}$, the cell lines H460, H520 and H661 irradiated with 20 Gy were treated for 24 h with 30 and 60 μM genistein and expression of $p21^{WAF1/CIP1}$ was studied. No effect on expression of $p21^{WAF1/CIP1}$ in H520 and H661 cells was seen, neither after irradiation with 20 Gy nor after treatment with 30 or 60 μM genistein. However, expression of $p21^{WAF1/CIP1}$ in H460 cells was increased from 0.5 to about 9 units/10^6 cells at 24 h following irradiation with 20 Gy, with an additional increase by 30 and 60 μM genistein to about 20 and 37 units/10^6 cells, respectively.

To alter cell-cycle progression after irradiation by another non-toxic method, the cell lines H460, H520 and H661 were irradiated with 20 Gy in S-phase and subcultured on agarose coated cell culture plates. Under both culture conditions, H460 and H520 cells showed a population doubling time of 1.8 days. In comparison, the proliferation of H661 cells with a doubling time of 2.1 days on plastic was inhibited on agarose with consecutive doubling times of >8 days. Analyses of cell-cycle progression of irradiated H661 cells have shown a delay of progression through the G1-and G2/M-phases (data not shown). Induction of apoptosis in H661 cultured on agarose was significantly ($p<0.0001$) reduced from 63.9±3.4% on plastic to 10.5±6.3% on agarose at day 6 post-irradiation, as measured by morphologic assessment of Hoechst 33342 stained cells. In addition, the hyperploid fraction of H661 cells cultured on agarose was also reduced from 27.9±3.1% on plastic to 9.6±1.6% on agarose as obtained by flow-cytometry. H520 and H460 cells, however, culturing on agarose did not lead to differences in cell-cycle progression, apoptosis and the fraction of hyperploid cell population. These data demonstrate that inhibition of cell-cycle progression can suppress the expression of radiation-induced apoptosis.

4. Discussion

In the absence of detailed knowledge of the critical molecular programs leading to radiation-induced apoptosis of NSCLC cells, the operational definition of apoptosis on the basis of common morphologic features of irreversible DNA degradation and fragmentation of the nucleus is widely used. One morphological characteristic of apoptosis is chromatin condensation into sharply circumscribed masses either marginated to the nuclear envelope or

pulverized into variegated aggregates (Wyllie *et al.* 1980, Earnshaw 1995, King and Cidlowski 1995). The aim of the present study was to characterize processes controlling the expression of morphological features of radiation-induced apoptosis in clonogenically inactivated NSCLC cell lines with or without functionally active p53. From the data of this study, a clear picture of the chain of events in NSCLC cells after irradiation emerged, that radiation-induced apoptosis is a late down-stream event secondary to cell-cycle progression. Apoptosis in irradiated NSCLC cells occurs late after the G2-phase block. Cell-cycle progression beyond G2/M is necessary and apoptosis cannot be enforced by increasing the amount of DNA damage in cells that have not progressed beyond G2/M. Cells with functionally active p53 pass beyond the G2 block with a markedly lower probability than cell lines with functionally inactive p53, during extended follow-up times of up to 144 h after irradiation in G1- or S-phase. They show a prolonged G2-phase block or to a lesser extent remain blocked in the G1-phase after irradiation in G1. As a consequence of this increased blockage, the apoptotic fraction induced in NSCLC with intact p53 was markedly lower than in cells with functionally inactive p53. In NSCLC cells without functional p53, apoptotic cells appeared from G2/M-phase cells showing the morphology of mitotic catastrophes, while p53-competent cells could complete mitosis and apoptosis appeared from G1′-phase cells. Together with apoptosis, hyperploid cells appeared in p53 competent and incompetent cells. In the latter, hyperploid cells apoptosed soon after generation. The appearance of cells showing the morphology of apoptosis could be prevented by caspase inhibitors.

Others have previously shown the appearance of radiation-induced late apoptosis in a temporal relation to the dissolution of the G2-phase block in lymphoid cell lines (Radford and Murphy 1994, Palayoor *et al.* 1995) and colorectal tumour cell lines (Bracey *et al.* 1997). In this context we added bivariate cytometry of a F-actin negativity and PI positivity, parameters related to apoptosis and DNA content and BrdU or ^{3}H incorporation in apoptotic cells to identify the cell cycle positions where individual cells apoptose. We found that apoptotic cells in H460 and A549 with active p53 come from the G1′-phase. In comparison, the majority of apoptotic H661 and H520 cells with non-functional p53 come from the G2/M-phase or at later times from the hyperploid cell population.

To analyse whether the traverse beyond the G2 block is a necessary prerequisite of radiation-induced apoptosis in NSCLC cell lines the G2 block was modulated. Caffeine, theophylline, 2-aminopurine and other drugs can reduce the G2-phase arrest and this can lead to an enhancement of radiation-induced apoptosis (Bracey *et al.* 1997, Palayoor *et al.* 1995, Bernhard *et al.* 1996). However, these drugs have a wide range of actions on cellular processes and can induce apoptosis in non-irradiated cells so it is hard to conclude that these drugs act solely by modulation of the G2 block on induction of apoptosis after irradiation. On the other hand, certain agents like TPA, forskolin and genistein could enhance the radiation-induced G2 block (Palayoor *et al.* 1995, Downes *et al.* 1992). In this study genistein was used to augment the G2 block of irradiated cells at non-toxic concentrations in NSCLC cell lines. Treatment of irradiated cell lines with genistein sustained the G2-phase arrest for longer periods and decreased the fraction of apoptotic cells in NSCLC cell lines with inactive p53. Arrest of cell-cycle progression with genistein was reported to be mediated by induced expression of $p21^{WAF1/CIP1}$ (Kuzumaki *et al.* 1998). This could not be observed in H520 and H661 cell lines so that the molecular pathways activated by genistein in these cell lines remains to be elucidated. In addition, the G2 block was prolonged by an independent method of plating cells on agarose. In H661, where cell-cycle progression and G2/M traverse was slowed down on agarose in comparison with plastic, induction of radiation-induced apoptosis was also diminished. This led to the conclusion, that radiation-induced late apoptosis is a down-stream event secondary to cell-cycle progression beyond the G2/M-phase arrest in NSCLC cell lines.

A key step in regulating the progression of cells through the G2/M-phase is activation of cdc2-cyclin B1 complexes (Nurse 1990, Jin *et al.* 1998). It was shown that DNA damage prevents the activation of cdc2-cyclin B1 complexes by a p53-mediated pathway (Jin *et al.* 1998). Chan *et al.* (1999) have shown that DNA damage leads to stabilization of p53, which was required for maintenance of the G2-phase arrest through activation of p21 and 14-3-3$_\sigma$. Inactivation of 14-3-3$_\sigma$ abrogates the G2-phase arrest and leads to migration of cdc2 and cyclin B1 to the nucleus (Chan *et al.* 1999). The premature entry of these cells containing damaged DNA into mitosis can lead to the apoptosis-like process of mitotic catastrophe, which is morphologically characterized by condensed and irregular fragmented chromosomes (Chan *et al.* 1999, Heald *et al.* 1993, Sit *et al.* 1997). Sit *et al.* (1997) showed that mitotic catastrophe can result from activation of apoptotic pathways by acute oxidative stress or direct endonuclease digestion in M-phase cells. Because M-phase apoptosis and mitotic catastrophes cannot be distinguished on a

morphological basis we included mitotic catastrophes as a subgroup of apoptosis. The fraction of cells with pulverized and condensed chromosomes, a major morphological characteristic of mitotic catastrophe found in chromosome preparations, was about 30% in cell lines with non-functional p53 at day 5 after irradiation. This was not found in the cell lines H460 and A549 with functional p53.

In addition to apoptosis, cells with a hyperploid DNA content (> G2) were generated after irradiation. Hyperploidy can be induced by releasing cells from the G2-phase arrest, via two main processes: (1) re-replication of the DNA in the absence of an intervening mitosis (Waldmann *et al.* 1996) or (2) in the absence of a functional spindle, a premature exit from mitosis to the next G1-phase without having completed chromatin migration to the poles (Kirsch-Volders *et al.* 1998, Verdoodt *et al.* 1999). The fraction of hyperploid cells among all post-G2 block cells were similar in all NSCLC cell lines irradiated in S regardless of their p53 function. P53 competent and incompetent NSCLC cells have about the same chance to become hyperploid after irradiation in S provided that they passed the G2 block. Thus, the pronounced G2 block in NSCLC cells protects cells from becoming hyperploid or apoptotic. Hyperploid cells from p53 competent cell lines were more apoptosis resistant in comparison with hyperploid cells from cell lines with non-functional p53. H661 and H520 cells irradiated in the G1-phase generate significantly higher fractions of hyperploid cells in comparison with irradiation in S-phase, irrespective if all cells or selectively all post-G2/M cells are regarded. Olive *et al.* (1996) have also shown that irradiation of lymphoblastoid cells with non-functional p53 in G1 generate a higher fraction of hyperploid cells when irradiated in G1-phase in comparison with irradiation in S-phase.

Radiation-induced G1- and G2-phase arrest points are considered to be periods of DNA repair and recovery (for a review, see Maity *et al.* 1997) and the amount of non-repaired DNA damage was attributed to play a key role in the induction of apoptosis (Aldridge and Radford 1998). In the present study, we considered whether markedly increasing the amount of residual DNA damage by inhibition of DNA double-strand break rejoining with wortmannin could influence the generation of apoptosis. While wortmannin efficiently increased the residual damage and concomitantly decreased the surviving fraction, as previously shown by Price and Youmell (1996) and Chernikova *et al.* (1999), no significant effect on apoptosis was seen in H460 and A549 with functional p53. These results also demonstrate that generation of apoptosis in heavily irradiated NSCL cell lines with 20 Gy could not be enforced by further increasing the prevalence of DNA damage.

In conclusion, radiation-induced apoptosis in NSCLC cells is a late removal mechanism of clonogenic inactivated cells secondary to cell-cycle progression beyond the G2 arrest point, unlike early interphase apoptosis mediated by p53, FAS/Apo-1/CD95 or sphingomyelin/ceramide pathways in other cell types after irradiation. The p53 protein blocks cell-cycle progression at G1- and G2/M-phases, which suppress subsequent p53-independent apoptosis. The generation of hyperploid cells is an alternative event to late apoptosis occurring in cells after the G2 block.

Acknowledgements

The authors thank Professor Dr G. Thiel (Institute for Medical Genetics, Charité, Berlin, Germany) for help with the *in-situ* hybridization technique, and Dr H. Schlechte (Clinic for Urology, Charité, Berlin, Germany) for help with the screening for mutations in p53. The research was supported by Grants Stu 151/4-4 from the Deutsche Forschungsgemeinschaft (DFG).

References

ALDRIDGE, D. R. and RADFORD, I. R., 1998, Explaining differences in sensitivity by ionizing radiation between human lymphoid cell lines. *Cancer Research*, **58,** 2817–2824.

BELKA, C., MARINI, P., BUDACH, W., SCHULZE-OSTHOFF, K., LANG, F., GULBINS, E. and BAMBERG, M., 1998, Radiation-induced apoptosis in human lymphocytes and lymphoma cells critically relies on the up-regulation of CD95/FAS/APO-1 ligand. *Radiation Research*, **149,** 588–595.

BENNET, M., MACDONALD, K., CHAN, S.-W., LUZIO, J. P., SIMARI, R. and WEISSBERG, P., 1998, Cell surface trafficking of Fas: a rapid mechanism of p53-mediated apoptosis. *Science*, **282,** 290–293.

BERNHARD, E. J., MUSCHEL, R. J., BAKANAUSKAS, V. J. and MCKENNA, W. G., 1996, Reducing the radiation-induced G2 delay causes HeLa cells to undergo apoptosis instead of mitotic deaths. *International Journal of Radiation Biology*, **69,** 575–584.

BRACEY, T. S., MILLER, J. C., PREECE, A. and PARASKEVA, C., 1995, γ-radiation-induced apoptosis in human colorectal adenoma and carcinoma cell lines can occur in the absence of wild-type p53. *Oncogene*, **10,** 2391–2396.

BRACEY, T. S., WILLIAMS, A. C. and PARASKEVA, C., 1997, Inhibition of radiation-induced G2 delay potentiates cell death by apoptosis and/or induction of giant cells in colorectal tumor cells with disrupted p53 function. *Clinical Cancer Research*, **3,** 1371–1381.

CHAN, T. A., HERMEKING, H., LENGAUER, C., KINZLER, K. W. and VOGELSTEIN, B., 1999, 14-3-3$_\sigma$ is required to prevent mitotic catastrophe after DNA damage. *Nature*, **401,** 616–620.

CHERNIKOVA, S. B., WELLS, R. L. and ELKIND, M. M., 1999,

Wortmannin sensitizes mammalian cells to radiation by inhibiting the DNA-dependent protein kinase-mediated rejoining of double-strand breaks. *Radiation Research*, **151,** 159–166.

CLARKE, A. R., GLEDHILL, S., HOOPER, M. L., BIRD, C. C., WYLLIE, A. H., 1994, p53 dependence of early apoptotic and proliferative responses within the mouse intestinal epithelium following γ-irradiation. *Oncogene*, **9,** 1767–1773.

CLARKE, A. R., PURDIE, C. A., HARRISON, D. J., MORRIS, R. G., BIRD, C. C., HOOPER, M. L. and WYLLIE, A. H., 1993, Thymocyte apoptosis induced by p53-dependent and independent pathways. *Nature*, **362,** 850–852.

DEWEY, W. C., LING, C. C. and MEYN, R., 1995, Radiation-induced apoptosis: relevance to radiotherapy. *International Journal of Radiation Oncology Biology Physics*, **33,** 781–796.

DOWNES, C. S., RYAN, A. and JOHNSON, R. T., 1992, Radiomimetic cell cycle delay induced by tetranodecanoyl phorbol acetate is enhanced by caffeine and by the protein kinase inhibitor 2-aminopurin. *International Journal of Radiation Biology*, **61,** 63–68.

EARNSHAW, W. C., 1995, Nuclear changes in apoptosis. *Current Opinion in Cellular Biology*, **7,** 337–343.

ENDRESEN, P. C., PRYTZ, P. S. and AARBAKKE, J., 1995, A new flow cytometric method for discrimination of apoptotic cells and detection of their cell cycle specificity through staining of F-actin and DNA. *Cytometry*, **20,** 162–171.

FRY, W. A., PHILLIPS, J. L. and MENCK, H. R., 1999, Ten-year survey of lung cancer treatment and survival in hospitals in the United States: a national cancer data base report. *Cancer*, **86,** 1867–1876.

GILLIGAN, D., MORT, C., MCMILLAN, T. J., PEACOCK, J. H., TITLEY, J. and ORMEROD, M. G., 1996, Application of a bromodeoxyuridine-Hoechst/ethidium bromide technique for the analysis of radiation-induced cell cycle delays in asynchronous cell populations. *International Journal of Radiation Biology*, **69,** 251–257.

HAIMOVITZ-FRIEDMAN, A., KAN, C.-C., EHLEITER, D., PERSAUD, R. S., MCLAUGHLIN, M., FUKS, Z. and KOLESNICK, N., 1994, Ionizing radiation acts on cellular membranes to generate ceramide and initiate apoptosis. *Journal of Experimental Medicine*, **180,** 525–535.

HASEGAWA, M., ZHANG, Y., NIIBE, H., TERRY, N. A. A. and MEISTRICH, M. L., 1998, Resistance of differentiating spermatogonia to radiation-induced apoptosis and loss in p53-dependent mice. *Radiation Research*, **149,** 263–270.

HEALD, R., MCLOUGHLIN, M. and MCKEON, F., 1993, Human Wee1 maintains mitotic timing by protecting the nucleus from cytoplasmatically activated cdc2 kinase. *Cell*, **74,** 463–574.

HERR, I., WILHELM, D., BÖHLER, T., ANGEL, P. and DEBATIN, K.-M., 1997, Activation of CD95(APO-1/Fas) signalling by ceramide mediates cancer therapy-induced apoptosis. *EMBO Journal*, **16,** 6200–6208.

JARVIS, W. D., KOLESNICK, R. N., FORNARI, F. A., TRAYLOR, R. S., GEWIRTZ, D. A. and GRANT, S., 1994, Induction of apoptotic DNA damage and cell death by activation of the sphingomyelin pathway. *Proceedings of the National Academy of Sciences, USA*, **91,** 73–77.

JIN, P., HARDY, S. and MORGAN, D. O., 1998, Nuclear localisation of cyclin B1 controls mitotic entry after DNA damage. *Journal of Cellular Biology*, **141,** 875–885.

KING, K. L. and CIDLOWSKI, J. A., 1995, Cell cycle and apoptosis: common pathways to life and death. *Journal of Cellular Biochemistry*, **58,** 175–180.

KIRSCH-VOLDERS, M., CUNDARI, E. and VERDOODT, B., 1998, Towards a unifying model for the metaphase/anaphase transition. *Mutagenesis*, **13,** 321–335.

KUZUMAKI, T., KOBAYASHI, T. and ISHIKAWA, K., 1998, Genistein induced $p21^{CIP1/WAF1}$ expression and blocks the G1 to S phase transition in mouse fibroblast and melanoma cells. *Biochemical and Biophysical Research Communications*, **157,** 183–189.

LOTEM, J. and SACHS, L., 1993, Hematopoitic cells from mice deficient in wild-type p53 are more resistant to induction of apoptosis by some agents. *Blood*, **82,** 1092–1096.

LOWE, S. W., SCHMITT, E. M., SMITH, S. W., OSBORNE, B. A. and JACKS, T., 1993, p53 is required for radiation-induced apoptosis in mouse thymocytes. *Nature*, **362,** 847–849.

MAITY, A., KAO, G. D., MUSHEL, R. J. and MCKENNA, W. G., 1997, Potential molecular targets for manipulating the radiation response. *International Journal of Radiation Biology*, **37,** 639–653.

MERRIT, A. J., ALLEN, T. D., POTTEN, C. S. and HICKMAN, J. A., 1997, Apoptosis in small intestinal epithelia from p53-null mice: evidence for a delayed, p53-independent G2/M-associated cell death after γ-irradiation. *Oncogene*, **14,** 2759–2766.

MERRIT, A. J., POTTEN, C. S., KEMP, C. J., HICKMAN, J. A., BALMAIN, A., LANE, D. P. and HALL, P. A., 1994, The role of p53 in spontaneous and radiation-induced apoptosis in the gastrointestinal tract of normal and p53-deficient mice. *Cancer Research*, **54,** 614–617.

MEYN, R. E., STEPHENS, L. C., ANG, K. K., HUNTER, N. R., BROCK, W. A., MILAS, L. and PETERS, L. J., 1993, Heterogeneity in the development of apoptosis in irradiated murine tumours of different histologies. *International Journal of Radiation Biology*, **64,** 583–591.

NURSE, P., 1990, Universal control mechanism regulating onset of M-phase. *Nature*, **397,** 104–105.

OLIVE, P. L., BANATH, J. P. and DURAND, R. E., 1996, Development of apoptosis and polyploidy in human lymphoblast cells as a function of position in the cell cycle at the time of irradiation. *Radiation Research*, **146,** 595–602.

OLIVE, P. L. and DURAND, R. E., 1997, Apoptosis: an indicator of radiosensitivity *in vitro*? *International Journal of Radiation Biology*, **71,** 695–707.

PALAYOOR, S. T., MACKLIS, R. M., BUMP, E. A. and COLEMAN, C. N., 1995, Modulation of radiation-induced apoptosis and G2/M block in murine T-lymphoma cells. *Radiation Research*, **141,** 235–243.

PENA, L. A., FUKS, Z. and KOLESNICK, R., 2000, Radiation-induced apoptosis of endothelial cells in the murine central nervous system: protection by fibroblast growth factor and sphingomyelinase deficiency. *Cancer Research*, **60,** 321–327.

PERDOMO, J. A., NAOMOTO, Y., HAISA, M., FUJIWARA, T., HAMADA, M., YASUOKA, Y. and TANAKA, N., 1998, *In vivo* influence of p53 status on proliferation and chemoradiosensitivity in non-small-cell lung cancer. *Journal of Cancer Research and Clinical Oncology*, **124,** 10–18.

PRICE, B. D. and YOUMELL, M. B., 1996, The phosphatidylinositol 3-kinase inhibitor wortmannin sensitizes murine fibroblasts and human tumor cells to radiation and blocks induction of p53 following DNA damage. *Cancer Research*, **56,** 246–250.

RADFORD, I. R., 1999, Review: Initiation of ionizing radiation-induced apoptosis: DNA damage-mediated or does ceramide have a role? *International Journal of Radiation Biology*, **75,** 521–528.

RADFORD, I. R. and MURPHY, T. K., 1994, Radiation response of mouse lymphoid and myeloid cell lines. Part 3. Different

signals can lead to apoptosis and may influence sensitivity to killing by DNA double-strand breakage. *International Journal of Radiation Biology*, **65,** 229–239.

SANTANA, P., PENA, L. A., HAIMOWITZ-FRIEDMAN, A., MARTIN, S., GREEN, D., MCLOUGHLIN, M., CORDON-CARDO, C., SCHUCHMAN, E. H., FUKS, Z. and KOLESNICK, R., 1996, Acid sphingomyelinase-deficient human lymphoblasts and mice are defective in radiation-induced apoptosis. *Cell*, **86,** 189–199.

SCHLECHTE, H. H., SCHNORR, D., LÖNING, T., RUDOLPH, B. D., POHRT, U. M. and LOENING, A., 1997, Mutation of the tumor suppressor gene p53 in human prostate and bladder cancers—investigation by temperature gradient gel electrophoresis (TGGE). *Journal of Urology*, **157,** 1049–1053.

SIRZEN, F., ZHIVOTOVSKY, NILSSON, A., BERGH, J. and LEWENSOHN, R., 1998, Spontaneous and radiation-induced apoptosis in lung carcinoma cells with different intrinsic radiosensitivities. *Anticancer Research*, **18,** 695–700.

SIT, K. H., YIN, L. and PARAMANANTHAM, R., 1997, Apoptotic condensation in M-phase cells. *Anatomical Record*, **248,** 149–158.

STAPPER, N. J., STUSCHKE, M., SAK, A. and STÜBEN, G., 1995, Radiation-induced apoptosis in human sarcoma and glioma cell lines. *International Journal of Cancer*, **62,** 58–62.

STRASSER, A., HARRIS, A. W., JACKS, T. and CORY, S., 1994, DNA damage can induce apoptosis in proliferating lymphoid cells via p53-independent mechanisms inhibitable by Bcl-2. *Cell*, **79,** 329–339.

TISHLER, R. B., CALDERWOOD, C. N., COLEMAN, C. N. and PRICE, B. D., 1993, Increases in specific DNA binding by p53 following treatment with chemotherapeutic and DNA damaging agents. *Cancer Research*, **53,** 2212–2216.

UBERTI, D., SCHWARTZ, D., ALMOG, N., GOLDFINGER, N., HARMELIN, A., MEMO, M. and ROTTER, V., 1999, Epithelial cells of different organs exhibit distinct patterns of p53-dependent and p53-independent apoptosis following DNA insult. *Experimental Cell Research*, **252,** 123–133.

VERDOODT, B., DECORDIER, I., GELEYNS, K., CUNHA, M., CUNDARI, E. and KIRSCH-VOLDERS, M. M., 1999, Induction of polyploid and apoptosis after exposure to high concentrations of the spindle poison nocodazole. *Mutagenesis*, **14,** 513–520.

WALDMANN, T., LENGAUER, C., KINZLER, K. W. and VOGELSTEIN, B., 1996, Uncoupling of S phase and mitosis induced by anticancer agents in cells lacking p21. *Nature*, **381,** 713–716.

WYLLIE, A. H., KERR, J. F. R. and CURIE, A. R., 1980, Cell death: the significance of apoptosis. *International Review of Cytology*, **68,** 251–306.

YANAGIHARA, K., NII, M., NUMOTO, M., KAMIYA, K., TAUCHI, H., SAWADA, S. and SEITO, T., 1995, Radiation-induced apoptotic cell death in human gastric epithelial tumour cells; correlation between mitotic death and apoptosis. *International Journal of Radiation Biology*, **67,** 677–685.

YONISH-ROUACH, E., RESNITZKY, D., LOTEM, J., SACHS, L., KIMCHI, A. and OREN, M., 1991, Wild-type p53 induces apoptosis of myeloid leukaemic cells that is inhibited by interleukin-6. *Nature*, **352,** 345–347.

ZHIVOTOVSKY, B., JOSEPH, B. and ORRENIUS, S., 1999, Tumor radiosensitivity and apoptosis. *Experimental Cell Research*, **248,** 10–17.